

Capping effects on spin and charge excitations in parent and superconducting $\text{Nd}_{1-x}\text{Sr}_x\text{NiO}_2$

S. Fan,^{1,*} H. LaBollita,² Q. Gao,³ N. Khan,⁴ Y. Gu,¹ T. Kim,¹ J. Li,¹ V. Bhartiya,¹ Y. Li,⁵ W. Sun,⁵ J. Yang,⁵ S. Yan,⁵ A. Barbour,¹ X. Zhou,^{3,6} A. Cano,⁷ F. Bernardini,⁸ Y. Nie,⁵ Z. Zhu,^{3,6} V. Bisogni,¹ C. Mazzoli,¹ A. S. Botana,² and J. Pelliciani^{1,†}

¹*National Synchrotron Light Source II, Brookhaven National Laboratory, Upton, NY 11973, USA.*

²*Department of Physics, Arizona State University, Tempe, AZ, USA.*

³*Institute of Physics and Beijing National Laboratory for Condensed Matter Physics, Chinese Academy of Sciences, Beijing 100190, China*

⁴*Department of Physics and Astronomy, Rutgers University, Piscataway, NJ 08854, USA.*

⁵*National Laboratory of Solid State Microstructures, Jiangsu Key Laboratory of Artificial Functional Materials,*

College of Engineering and Applied Sciences, Nanjing University, Nanjing, China 210046

⁶*Songshan Lake Materials Laboratory, Dongguan 523808, China*

⁷*CNRS, Université Grenoble Alpes, Institut Néel, 38042 Grenoble, France*

⁸*Dipartimento di Fisica, Università di Cagliari, IT-09042 Monserrato, Italy*

Superconductivity in infinite layer nickelates $\text{Nd}_{1-x}\text{Sr}_x\text{NiO}_2$ has so far been achieved only in thin films raising questions on the role of substrates and interfaces. Given the challenges associated with their synthesis it is imperative to identify their intrinsic properties. We use Resonant Inelastic X-ray Scattering (RIXS) to investigate the influence of the SrTiO_3 capping layer on the excitations of $\text{Nd}_{1-x}\text{Sr}_x\text{NiO}_2$ ($x = 0$ and 0.2). Spin excitations are observed in parent and 20% doped $\text{Nd}_{1-x}\text{Sr}_x\text{NiO}_2$ regardless of capping, proving that magnetism is intrinsic to infinite-layer nickelates and appears in a significant fraction of their phase diagram. In parent and superconducting $\text{Nd}_{1-x}\text{Sr}_x\text{NiO}_2$, the spin excitations are slightly hardened in capped samples compared to the non-capped ones. Additionally, a weaker Ni - Nd charge transfer peak at ~ 0.6 eV suggests that the hybridization between Ni $3d$ and Nd $5d$ orbitals is reduced in capped samples. From our data, capping induces only minimal differences in $\text{Nd}_{1-x}\text{Sr}_x\text{NiO}_2$ and we phenomenologically discuss these differences based on the reconstruction of the SrTiO_3 - NdNiO_2 interface and other mechanisms such as crystalline disorder.

The search for cuprate analog materials has led to the discovery of superconductivity in infinite layer (RNiO_2), quintuple-layer ($\text{Nd}_6\text{Ni}_5\text{O}_{12}$), and bilayer ($\text{La}_3\text{Ni}_2\text{O}_7$) nickelates [1–3]. Infinite layer nickelates RNiO_2 ($\text{R}=\text{Nd}$, Pr , and La) are weak insulators composed of NiO_2 planes lacking apical oxygens separated by rare-earth (R) layers [Fig. 1(a)] [1, 4–7]. In undoped RNiO_2 , nickel has a nominal Ni^{1+} oxidation state, a d^9 electronic configuration, and $d_{x^2-y^2}$ orbital polarization similar to parent cuprates, and once hole-doped, RNiO_2 displays superconductivity [1]. Resonant Inelastic X-ray Scattering (RIXS) detected dispersive spin excitations with $J \approx 64$ meV [8] in capped NdNiO_2 significantly lower in energy than in cuprates [9–11], whereas, in uncapped NdNiO_2 , a peak at $\approx (1/3, 0, L)$ r. l. u. concomitant with the absence of spin excitations was reported and a charge ordered ground state was inferred [8, 12–17]. From a synthesis perspective, superconductivity of RNiO_2 has so far been detected only in thin films, a key distinction from cuprates [4–7, 18] which raises questions on the role of substrate, capping, and interface.

In the past, multiple phenomena have been observed

at the interface of oxide thin films as due to the combination of polar/non-polar surfaces, charge transfer, phonon coupling, confinement and strain, among others [19–26]. These interface modifications can affect a large portion of the film due to either the limited thickness or long-range interactions [26–29]. Electron-energy loss spectroscopy (EELS) and scanning transmission electron microscopy (STEM) revealed a thickness-dependent atomic and electronic reconstruction at the NdNiO_2 - SrTiO_3 interface, the effects of which can propagate to the inner NiO_2 layers [30, 31]. Relevant to the presence or absence of capping the following evidence can be extracted: (i) capping modifies the distribution of apical oxygen during the chemical reduction [15, 30, 32]; (ii) a $q = (1/3, 0, L)$ peak (which was assigned as the charge density wave) is detected in uncapped nickelates with weak or absent spin excitations [12, 13, 16, 17, 32]; and (iii) superconductivity is observed in both capped and uncapped cases with some sample-specific differences in T_C [13, 33–41]. However, experimental information on the capping layer and its repercussion on the electronic and magnetic excitations have still to be explored using high-end spectroscopies.

Here we combine X-ray Absorption Spectroscopy (XAS) and high-resolution RIXS to investigate the electronic excitations of $\text{Nd}_{1-x}\text{Sr}_x\text{NiO}_2$ ($x = 0, 0.2$) as a

* sfan1@bnl.gov

† pelliciani@bnl.gov

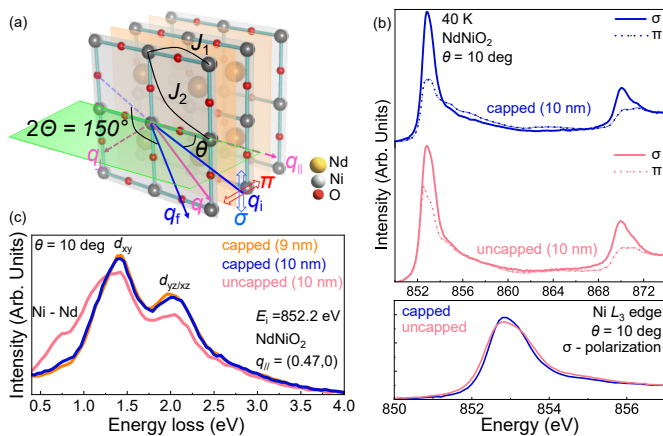


FIG. 1. (a) Geometry of XAS and RIXS. \vec{q}_i and \vec{q}_f represent the wave-vectors of incident and scattered X-rays. The grazing angle θ is defined as the angle between the incident x-ray and the sample surface. The 2θ scattering angle (angle between \vec{q}_i and \vec{q}_f) is fixed at 150 degrees to maximize the momentum transfer. \vec{q}_{\parallel} and \vec{q}_{\perp} refer to that the momentum transfer direction is parallel or perpendicular to the Ni-O bonds, respectively. (b) XAS linear dichroism of the NdNiO₂ - cap and NdNiO₂ - uncap (both 10 nm) at Ni L_3/L_2 edges. The grazing angle θ is 10 deg. Bottom: comparison of XAS of the NdNiO₂ - cap/uncap at the Ni L_3 edge with σ -polarization. (c) RIXS spectra of the NdNiO₂ - cap/uncap with $\theta = 10$ deg, σ -polarization, and $E_i = 852.2$ eV.

function of Sr doping and in the presence/absence of the SrTiO₃ capping layer. High quality Nd_{1-x}Sr_xNiO₂ display strong orbital polarization and spin excitations are detected regardless of capping. Strontium doping softens the spin excitations due to magnetic dilution achieved through hole doping on the nickel site [8, 37]. Furthermore, spin excitation energies of the capped parent and superconducting compounds are slightly increased compared to the uncapped counterparts. A suppressed charge transfer peak at ~ 0.6 eV in capped samples indicates that capping reduces the hybridization between Ni $3d$ and Nd $5d$ orbitals. This evidence proves that magnetism is an intrinsic property of infinite layer nickelates and that capping has only minor effects on the spin and charge excitations in infinite-layer nickelate films.

We studied: (i) NdNiO₂ with and without capping (NdNiO₂ - cap/uncap, 10 nm thick) and (ii) Nd_{0.8}Sr_{0.2}NiO₂ with and without capping (Nd_{0.8}Sr_{0.2}NiO₂ - cap/uncap). The thickness of the SrTiO₃ capping layer is 3 nm for both parent and doped films. All films are grown on SrTiO₃ [42]. A 9 nm NdNiO₂ - cap is also measured for comparison. The high sample quality is confirmed by resonant x-ray diffraction (See End Matter), electric transport, and X-ray absorption measurements at the Ni- L and O- K edges. The T_C of the doped samples is 11 and 15 K for Nd_{0.8}Sr_{0.2}NiO₂ - uncap and Nd_{0.8}Sr_{0.2}NiO₂ - cap, respectively (Supplementary Fig. 2). We perform XAS

at the Ni L_3/L_2 edges in total electron yield (TEY) and RIXS at the Ni L_3 edge with σ - and π -polarization using the experimental geometry sketched in Fig. 1(a). At $\theta = 10$ degree, the σ - or π - x-ray polarization refers to the electric field vector of the light being along the in-plane Ni-O bond direction or almost along the out-of-plane direction, respectively.

Figure 1(b) displays the XAS linear dichroism of NdNiO₂ - cap and NdNiO₂ - uncap. The XAS corroborates the high quality of our samples as they display a single peak in σ -polarization (bottom panel) and strong linear dichroism (ΔI) regardless of capping [43]. This implies an in-plane orientation of the unoccupied Ni $3d_{x^2-y^2}$ orbitals [37, 44]. The XAS dichroism is sensitive to the presence of spurious phases [15, 32] because the excess apical oxygen in the partially reduced films deplete the anisotropic polarization of the in- and out-of-plane Ni $3d$ orbitals. This indicates that our samples have minimal spurious signals from secondary phases [15]. The peak in σ -polarization (≈ 852.3 eV) corresponds to the Ni $2p^63d^9 \rightarrow 2p^53d^{10}$ transition related to Ni¹⁺ valence state. In π -polarization, a weak shoulder emerges around 853 eV for uncapped NdNiO₂ and is ascribed to the Ni²⁺ state originating from self-doping induced by Ni-Nd orbital hybridization [8, 45]. Since the Ni-Nd hybridization is mainly along the out-of-plane direction, the Ni²⁺ is more prominent in the π -polarized XAS. This is confirmed by the RIXS spectra displayed in Fig. 1(c) where the Nd $5d$ - Ni $3d$ charge transfer peak at ≈ 0.6 eV is moderately suppressed in the NdNiO₂ - cap. Similar capping effects are also consistently observed in the XAS and RIXS spectra of the Nd_{0.8}Sr_{0.2}NiO₂ (Supplementary Fig. 3).

Figure 2(a) shows RIXS spectra at low-energy loss ($-100 \rightarrow 400$ meV) in σ -polarization for all the samples at $q_{\parallel} = (0.36, 0)$ r. l. u.. Besides the elastic line, a phonon at ≈ 60 meV and a dispersive spin excitation at 100 - 200 meV are clearly identified [8]. We fit the data with a Gaussian peak for the elastic and phonon while the spin excitations are fitted via a damped harmonic oscillator [8, 11] (see Supplementary Information section IV for details). The background is fitted by a broad anti-symmetric Lorentzian function capturing the decay from Ni dd excitations. After the removal of the elastic peak, the RIXS data are summarized in Fig. 2(b-e) for $(h, 0)$ and (h, h) . The dispersive color bands above 100 meV in NdNiO₂ - cap/uncap provide robust evidence on the presence of spin excitations in NdNiO₂ irrespective of capping. This observation is at odds with Ref. 13, where spin excitations are absent for NdNiO₂ - uncap. The inconsistency is likely due to distinct sample quality as the XAS look significantly different and we could not observe any resonant peak at $q = (1/3, 0, L)$ (see ‘End Matter’) [13, 15, 32]. The spin excitations persist in hole-doped samples and their bandwidth softens and intensities are suppressed due to the reduction of exchange bonds induced by hole doping on the nickel sites [Fig. 2 (c,e)].

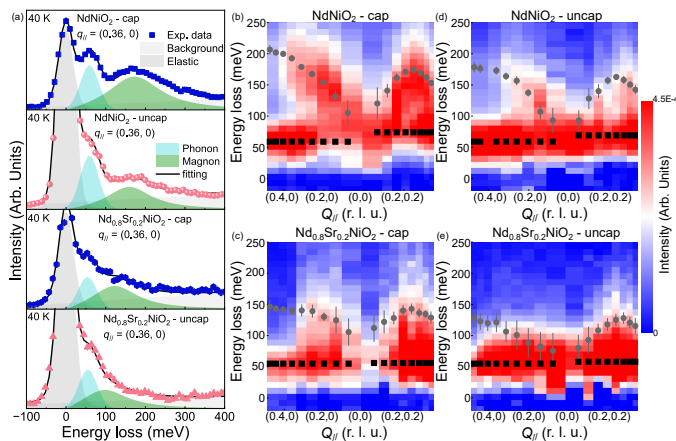


FIG. 2. (a) RIXS spectra for NdNiO_2 - cap, NdNiO_2 - uncap, $\text{Nd}_{0.8}\text{Sr}_{0.2}\text{NiO}_2$ - cap and $\text{Nd}_{0.8}\text{Sr}_{0.2}\text{NiO}_2$ - uncap at 40 K and $q_{\parallel} = (0.36, 0)$ r. l. u. in σ -polarization. The spectra are fitted using three peaks. Light grey represents the background. (b,d) RIXS intensity map vs. energy loss and in-plane momentum transfer along $(h, 0)$ and (h, h) of the NdNiO_2 - cap/uncap, respectively. (c,e) Similar RIXS intensity map as (b,d) but for the $\text{Nd}_{0.8}\text{Sr}_{0.2}\text{NiO}_2$ - cap/uncap, respectively. Grey and black data points correspond to the phonon and spin excitation dispersions extracted from the fitting.

This doping trend seems to be intrinsic of the samples proving the magnetic dilution effect due to hole doping regardless of capping.

Figure 3(a) compares the spin excitations' energy of NdNiO_2 - cap and NdNiO_2 - uncap. To quantify the spin dispersion we use linear spin wave theory for the spin 1/2 square-lattice Heisenberg antiferromagnet [8, 46]:

$$H = J_1 \sum_{i,j} S_i \cdot S_j + J_2 \sum_{i,i'} S_i \cdot S_{i'} \quad (1)$$

where S_i , S_j , and $S_{i'}$ are spins at site i , nearest-neighbor sites j , and the next nearest-neighbor sites i' , respectively. J_1 and J_2 are the nearest and second-nearest exchange constants [Fig. 1(a)] [8]. We obtained $J_1 \approx 72.8 \pm 4.3$ meV and $J_2 \approx -5.8 \pm 2.0$ meV in the NdNiO_2 - cap (10 nm), consistent with previous studies [8] and for the NdNiO_2 - uncap, $J_1 \approx 67.0 \pm 4.0$ and $J_2 \approx -5.2 \pm 2.0$ meV. The spin excitation energy of NdNiO_2 - cap is systematically higher than that of the uncapped case at all the significant momentum points. We believe that this hardening is intrinsic given that the spin excitation energies are nearly identical for 9 and 10 nm thick NdNiO_2 - cap (which we used to identify the sample-to-sample variations). Besides the value of J_s , the capping-induced hardening of the spin excitations can be more directly identified in the raw RIXS spectra at high momentum (see End Matter). A similar behavior of the spin excitations hardening in presence of capping is also detected in $\text{Nd}_{0.8}\text{Sr}_{0.2}\text{NiO}_2$ [Fig. 3(b)]. In doped films, J_2 is set to

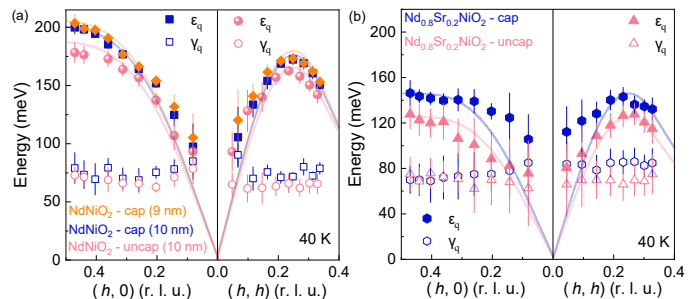


FIG. 3. (a,b) Fitted un-damped spin excitation energy ϵ_q and damping factor γ_q as a function of in-plane momentum transfer along $(h, 0)$ and (h, h) of NdNiO_2 - cap/uncap (a) and superconducting $\text{Nd}_{0.8}\text{Sr}_{0.2}\text{NiO}_2$ - cap/uncap (b). The curves in light colors are the spin excitation dispersion from linear spin wave theory. The data of the 9 nm NdNiO_2 - cap is also added for comparison.

zero to avoid overfitting due to the reduced bandwidth of the spin excitations.

Our data highlights that magnetism is intrinsic to $\text{Nd}_{1-x}\text{Sr}_x\text{NiO}_2$ and that the SrTiO_3 capping layer has overall minor effects on the spin and charge excitations. Importantly, the strong XAS dichroism, absence of any pre-edge peak at the O-K edge (see End Matter), lack of the resonant $q = (1/3, 0, L)$ peak (see End Matter), and presence of similar spin excitations in our capped and uncapped films demonstrate that the quality of our capped and uncapped samples is comparable. Therefore, we tend to interpret the slightly renormalized spin excitation energy and weakening of the Nd - Ni hybridization upon capping as a combination of effects such as interfacial reconstruction, crystalline defects, or lattice disorder [30, 31, 39, 47, 48].

One of the important aspects is the atomic and electronic reconstruction at the SrTiO_3 - NdNiO_2 interface due to polar discontinuity [28–31, 33–36, 39]. However, how the SrTiO_3 - NdNiO_2 interface affects the electronic properties of the inner bulk-like NdNiO_2 layers upon capping is still underexplored. Previous work reported that an intermediate layer such as $\text{Nd}(\text{Ti},\text{Ni})\text{O}_3$ forms, which increases the topotactic reduction energy [31]. Therefore, apical oxygen can be present at the interface shifting the Ni atoms renormalizing the Ni-Nd and Ni-O orbital hybridization [31]. The interfacial atomic reconstruction has been proved to affect the electronic structure of nickelates for about 5 - 6 layers (~ 2 nm) [30, 31]. Since the x-ray penetration depth (hundreds of nanometers) is much larger than the film thickness, the RIXS signal related to atomic and electronic reconstruction is about 20% volume of our measured films ($c = 3.31 \text{ \AA}$).

To better understand how the interface renormalization affects the electronic properties of the bulk-like NiO_2 layers, we compute the atom- and layer-resolved density of states (DOS) of NdNiO_2 - cap and NdNiO_2 - uncap. We calculate the most thermodynamically stable

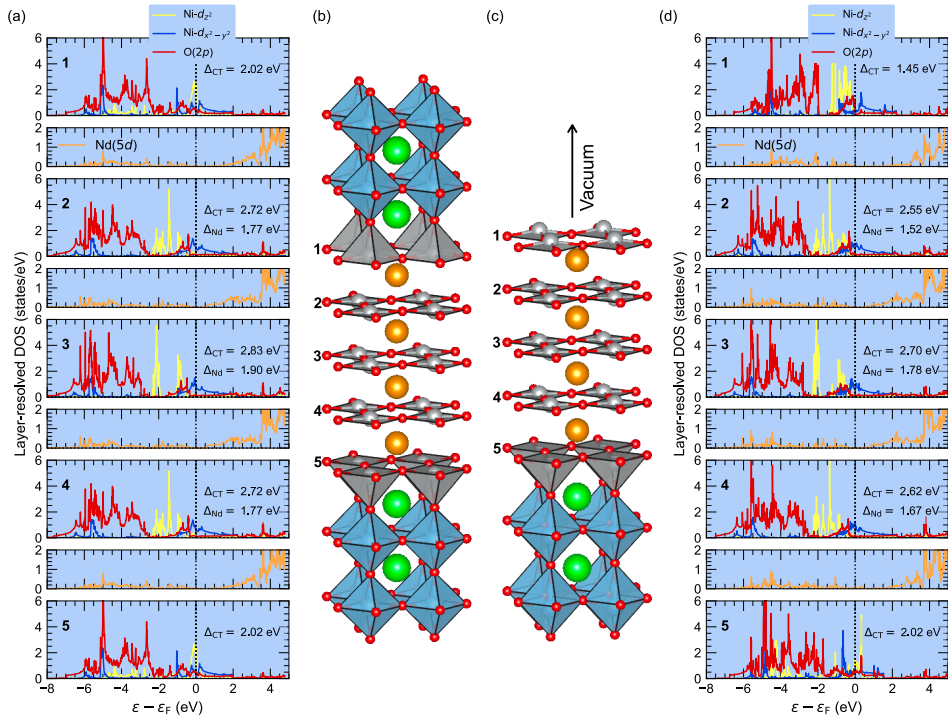


FIG. 4. Summary of the “capping” vs. “uncapping” effects on the electronic structure of SrO interface for NdNiO₂. (a) Layer- and atom-resolved density of states (DOS) within the NdNiO₂ block in the “capped” NdNiO₂ with focus on the Nd(5*d*), O(2*p*), and Ni-*e_g* states. (b) Crystal structure of NdNiO₂/SrTiO₃ heterostructure with SrO interface which refers to a “capped” NdNiO₂. (c) Same as (b) for the “uncapped” case. (d) Same as (a) for the “uncapped” case.

SrO-type of the interface (Supplementary Fig. 9) [36] and the calculation considers five NiO₂ layers. Figure 4 displays the DOS of the Ni 3*d*, Nd 5*d*, and O 2*p* orbitals of the NdNiO₂ - cap and NdNiO₂ - uncap. As expected, the most significant effects of “capping” manifest in the interfacial layer (layer 1), where the charge-transfer energy between Ni 3*d* and O 2*p* states is substantially enhanced compared to the “uncapped” scenario. Remarkably, the electronic renormalization from the interface also influences the inner NiO₂ layers. The calculations with “capping” capture the decreased hybridization between the Ni 3*d* and Nd 5*d* states, evident in a larger Ni - Nd charge transfer energy (Δ_{Nd}) consistent with experimental results [Fig. 1(c)]. This reveals that “capping” can indeed affect the electronic properties of NdNiO₂ and the effects are not limited to the SrTiO₃-NdNiO₂ interface.

The magnetic behavior could also be rationalized by the interface effects. As the Ni-Nd and Ni-O orbital hybridization decreases upon “capping”, less Ni²⁺ states are present. This reduces the effective self-hole doping in the nickel site which hardens the spin excitations for the NdNiO₂ - cap. However, although the electronic renormalization can propagate to 5-6 NiO₂ layers into the film, the difference of the Ni-Nd hybridization between the NdNiO₂ - cap and NdNiO₂ - uncap is overall small since our film thickness is 10 nm which is larger than the length scale of the interface propagation effects. This is

consistent with a minor renormalization of the spin excitation energy due to capping [Fig. 3(a)].

Although the physical picture of the electronic renormalization induced by the interface is phenomenologically consistent with our data, we cannot fully disregard the effects from lattice or crystalline disorder (not the impurity phases like Nd₃Ni₃O₇ or Nd₃Ni₃O₈) due to the common challenges of synthesizing infinite-layer nickelate films [31, 32]. Previous RIXS studies on infinite-layer cuprates (SrCuO₂)_{*n*}/(SrTiO₃)₂ suggested that the spin excitations can be renormalized due to the reorientation of the copper-oxygen plaquettes below the critical thickness caused by a relaxation of the polar electrostatic energy [47]. The disordered states form scattering points for spin excitations, which quench the spectral weight of the spin excitations but do not change their overall bandwidth [47]. Our data could also be captured within this picture. However, it remains difficult to disentangle the impact of crystalline defects, strain relaxation, oxygen vacancy, cation structure and lattice disorder as they can vary from sample to sample which deserves future dedicated investigation.

In summary, we investigated the capping effects on the electronic spectra of infinite-layer nickelates. In Nd_{1-x}Sr_xNiO₂ (*x* = 0, 0.2), strong orbital polarization and spin excitations are present regardless of capping. We specifically identified that capping slightly hardens

the spin excitation and weakens the Ni - Nd orbital hybridization. While our results can be phenomenologically rationalized by a combination of effects such as interface renormalization, crystal defects and lattice disorder, the x-ray data proves the intrinsic robustness of spin excitations in the phase diagram of infinite layer nickelates similarly to cuprates.

ACKNOWLEDGEMENTS

We thank Dr. Mark Dean and Dr. John Tranquada for fruitful discussions. Work at Brookhaven National Laboratory was supported by the DOE Office of Science under Contract No. DE-SC0012704. This work was supported by the Laboratory Directed Research and Development project of Brookhaven National Laboratory No. 21-037. This work was supported by the U.S. Department of Energy (DOE) Office of Science, Early Career Research Program. This research used beamline 2-ID SIX and 23-ID-1 CSX of the National Synchrotron Light Source II, a U.S. Department of Energy (DOE) Office of Science User Facility operated for the DOE Office of Science by Brookhaven National Laboratory under Contract No. DE-SC0012704. We also acknowledge resources made available through BNL/LDRD No. 19-013. The work at IOP is supported by the National Natural Science Foundation of China (Grant Nos. 12074411 and 11888101), Strategic Priority Research Program (B) of the Chinese Academy of Sciences (Grant No. XDB25000000). Y.N. would like to acknowledge the funding support from the National Natural Science Foundation of China (Grant Nos. 11861161004 and 11774153). ASB and AC acknowledge the LANEF chair of excellence. HL was supported by NSF Grant No. DMR 2045826.

Competing interest: The authors declare no competing interests.

END MATTER

High-quality of NdNiO₂ - uncap films

XAS at the O-*K* edge is sensitive to the Nd₃Ni₃O₇ or Nd₃Ni₃O₈ impurity phases and we therefore use it to establish the quality of our samples [15, 32]. Figure 5(a) shows the XAS of the NdNiO₂ - uncap at the O-*K* edge. Despite small intensity variation, the spectrum displays nearly identical peaks to SrTiO₃ without any pre-edge peak due to the Ni-O hybridization as in NdNiO₃ [15, 45]. This pre-edge peak is also observed in partially reduced films with reduced intensity compared to NdNiO₃ [32]. This result proves that our film is fully or mostly reduced.

Figure 5(b) shows the XAS linear dichroism at the Ni *L*₃/*L*₂ edges of the superconducting Nd_{0.8}Sr_{0.2}NiO₂ -

cap/uncap. Both capped and uncapped samples display strong dichroism at the Ni *L*₃ and *L*₂ edges, demonstrating a strong anisotropic orbital polarization in Sr-doped NdNiO₂. The strong XAS linear dichroism of parent and doped NdNiO₂ regardless of capping demonstrates the high quality of our entire sample sets and the minimal self-doping effect.

To further prove the quality of our NdNiO₂ - uncap, we perform resonant x-ray diffraction (RXRD) on NdNiO₂ - uncap and on bare SrTiO₃. Figure 5(c) displays the RXRD intensity along the (*h*, 0, 0.29) direction of NdNiO₂ - uncap and SrTiO₃. In both cases, we observe a peak at *h* = 0.33 which can be indexed with the Bragg peak of SrTiO₃ (101) emerging from the third harmonic contamination of the beamline [14]. This is proved by the lack of any resonant enhancement across the Ni *L* edge displayed in Fig. 5(d). The lack of resonance corroborates that this peak is structural and that the indexation shows that it originates from the substrate. Minor differences of the (0.33, 0, 0.29) peak between the NdNiO₂ - uncap and SrTiO₃ are due to the different reflectivity caused by the presence of interfaces between the substrate and the film.

The resonant *q* = (1/3, 0, *L*) peak detected in other work [15] is not detected in our uncapped NdNiO₂. Because of the extremely strong intensity of the intermediate Nd₃Ni₃O₇/Nd₃Ni₃O₈ phase when on-resonance, the *q* = (1/3, 0, *L*) peak is detectable even if small amounts of the partially reduced phase are present [15]. Therefore, the absence of such a peak in our NdNiO₂ - uncap demonstrates that our samples are free of the impurity phases [15, 32].

Error bar estimation and sample-to-sample variation

The exchange constants in the different nickelates are determined by calculating the smallest χ^2 from different combination of *J*₁ and *J*₂ values using linear spin-wave theory. The χ^2 is directly related to the variance between the theory and the experimental spin excitation dispersion:

$$\chi^2 = \sum_{q_i}^{q_f} \frac{[\epsilon_{q_i}^{exp} - \epsilon_{q_i}^{cal}]^2}{\epsilon_{q_i}^{cal}} \quad (2)$$

where *q*_{*i*} and *q*_{*f*} refer to the transferred momenta near the antiferromagnetic zone center and zone boundary, respectively. $\epsilon_{q_i}^{exp}$ and $\epsilon_{q_i}^{cal}$ are the experimental and calculated spin excitations energies at a specific momentum point. We keep the same ratio of *J*₁/*J*₂ for both NdNiO₂ - cap and NdNiO₂ - uncap to further constrain the fitting. Furthermore, due to the large uncertainties caused by the overlap between phonon and spin excitations at *q*_{||} < 0.2 r. l. u., we remove the last two *q* points. Using

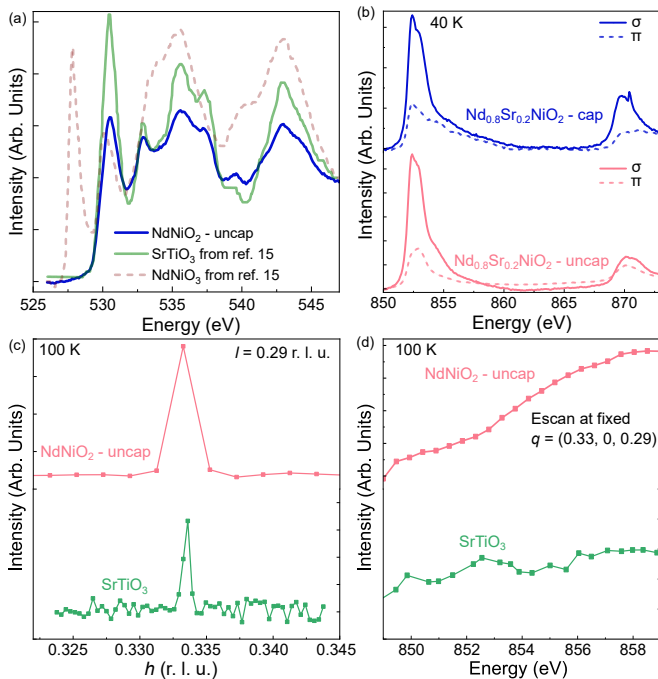


FIG. 5. (a) XAS comparison at the O- K edge of the NdNiO_2 - uncap, the SrTiO_3 , and perovskite NdNiO_3 . The data of SrTiO_3 and NdNiO_3 grown on the SrTiO_3 substrate are reproduced from Ref. 15. (b) XAS linear dichroism of the superconducting $\text{Nd}_{0.8}\text{Sr}_{0.2}\text{NiO}_2$ - cap/uncap at the Ni L_3 and L_2 edge. The sharp feature at about 870 eV in the σ -polarized XAS of the $\text{Nd}_{0.8}\text{Sr}_{0.2}\text{NiO}_2$ - cap is a spike of the detector. (c) The Resonant x-ray diffraction (RXRD) scan along the $(h, 0, 0.29)$ direction of the NdNiO_2 - uncap and the bare SrTiO_3 substrate at $E_i = 854$ eV. (d) RXRD intensity as a function of incident x-ray energy of NdNiO_2 - uncap and SrTiO_3 at fixed $q = (0.33, 0, 0.29)$ r. l. u. across the Ni L_3 edge. The background fluorescence was subtracted. The RXRD measurements were taken at 100 K.

this method, we obtain $J_1 = 72.8 \pm 4.3$ meV and $J_2 = -5.8 \pm 2.0$ meV for the 10 nm NdNiO_2 - cap, and $J_1 = 67.0 \pm 4.0$ meV and $J_2 = -5.2 \pm 2.0$ meV for the 10 nm NdNiO_2 - uncap.

Considering the overall error bars, it is difficult to visualize the precise change of J_1 and J_2 due to capping. However, in Fig. 3 the bandwidth of spin excitation is systematically increased in capped samples for all momentum points. On the contrary, the spin excitation energies are nearly identical for 9 and 10 nm thick NdNiO_2 - cap. This proves that the capping induced spin excitation hardening is measurable, even if hardly quantifiable, and not due to sample-to-sample variations.

Figure 6(a) shows the comparison of the raw RIXS spectra of NdNiO_2 - cap and NdNiO_2 - uncap at $q = (0.47, 0)$ r. l. u., where spin excitations and phonon are well-separated. While the phonon remains at the same energy, capping hardens the spin excitation by about 20 meV. Figure 6(b) displays the comparison of the raw RIXS spectra of 9 and 10 nm NdNiO_2 - cap. The spin

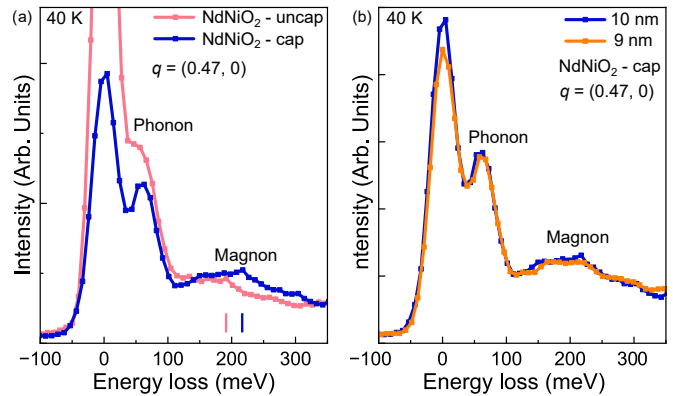


FIG. 6. (a) Comparison of the RIXS spectra of NdNiO_2 - cap and NdNiO_2 - uncap. The vertical lines indicate the spin excitation energies. (b) Comparison of the RIXS spectra of 9 and 10 nm NdNiO_2 - cap.

excitations are nearly unchanged. This evidence shows that the capping-induced spin excitation hardening is significant compared to the level of sample-to-sample variations.

- [1] D. Li, L. K., B. Y. Wang, M. Osada, S. Crossley, H. R. Lee, Y. Cui, Y. Hikita, and H. Y. Hwang, *Nature* **572**, 624 (2019).
- [2] G. A. Pan, D. F. Segedin, H. LaBollita, Q. Song, E. M. Nica, B. H. Goodge, A. T. Pierce, S. Doyle, S. Novakov, D. C. Carrizales, A. T. N. P. Shafer, H. Paik, J. T. Heron, J. A. Mason, A. Yacoby, L. F. Kourkoutis, O. Erten, C. M. Brooks, A. S. Botana, and J. A. Mundy, *Nat. Mater.* **1**, 5 (2021).
- [3] H. Sun, M. Huo, X. Hu, J. Li, Z. Liu, Y. Han, L. Tang, Z. Mao, P. Yang, B. Wang, J. Cheng, D. Yao, G. Zhang, and M. Wang, *Nature* (2023), <https://doi.org/10.1038/s41586-023-06408-7>.
- [4] Q. Li, C. He, J. Si, X. Zhu, Y. Zhang, and H. H. Wen, *Commun. Mater.* **1**, 16 (2020).
- [5] K. Lee, B. H. Goodge, D. Li, M. Osada, B. Y. Wang, Y. Cui, L. F. Kourkoutis, and H. Y. Hwang, *APL Materials* **8**, 041107 (2020), publisher: American Institute of Physics.
- [6] B.-X. Wang, H. Zheng, E. Krivyakina, O. Chmaissem, P. P. Lopes, J. W. Lynn, L. C. Gallington, Y. Ren, S. Rosenkranz, J. F. Mitchell, and D. Phelan, *Physical Review Materials* **4**, 084409 (2020), publisher: American Physical Society.
- [7] P. Puphal, Y.-M. Wu, K. Fürsich, H. Lee, M. Pakdaman, J. A. N. Bruin, J. Nuss, Y. E. Suyolcu, P. A. van Aken, B. Keimer, M. Isobe, and M. Hepting, *Science Advances* **7**, eabl8091, publisher: American Association for the Advancement of Science.
- [8] H. Lu, M. Rossi, A. Nag, M. Osada, D. F. Li, K. Lee, B. Y. Wang, M. Garcia-Fernandez, S. Agrestini, Z. X. Deann, E. M. Been, B. Moritz, T. P. Devereaux, J. Zaanen, H. Y. Hwang, K.-J. Zhou, and W. S. Lee, *Science* **373**, 213 (2021).

- [9] L. Braicovich, L. J. P. Ament, V. Bisogni, F. Forte, C. Aruta, G. Balestrino, N. B. Brookes, G. M. De Luca, P. G. Medaglia, F. Miletto Granozio, M. Radovic, M. Salluzzo, J. van den Brink, and G. Ghiringhelli, *Phys. Rev. Lett.* **102**, 167401 (2009).
- [10] M. Le Tacon, G. Ghiringhelli, J. Chaloupka, M. Moretti Sala, V. Hinkov, M. W. Haverkort, M. Minola, M. Bakr, K. J. Zhou, S. Blanco-Canosa, C. Monney, Y. T. Song, G. L. Sun, C. T. Lin, G. M. De Luca, M. Salluzzo, G. Khaliullin, T. Schmitt, L. Braicovich, and B. Keimer, *Nature Phys.* **7**, 725 (2011).
- [11] Y. Y. Peng, W. Huang, E., R. Fumagalli, M. Minola, Y. Wang, X. Sun, Y. Ding, K. Kummer, X. J. Zhou, N. B. Brookes, B. Moritz, L. Braicovich, T. P. Devereaux, and G. Ghiringhelli, *Phys. Rev. B.* **98**, 144507 (2018).
- [12] M. Rossi, M. Osada, J. Choi, S. Agrestini, D. Jost, Y. Lee, H. Lu, B. Y. Wang, K. Lee, A. Nag, Y. D. Chuang, C. T. Kuo, S. J. Lee, B. Moritz, T. P. Devereaux, Z. X. Shen, J. S. Lee, K. J. Zhou, H. Y. Hwang, and W. Lee, *Nat. Phys.* **18**, 869 (2022).
- [13] G. Krieger, L. Martinelli, S. Zeng, L. E. Chow, K. Kummer, R. Arpaia, M. Moretti Sala, N. B. Brookes, A. Ariando, N. Viart, M. Salluzzo, G. Ghiringhelli, and D. Preziosi, *Phys. Rev. Lett.* **129**, 027002 (2022).
- [14] J. Pellicciari, N. Khan, P. Wasik, A. Barbour, Y. Li, Y. Nie, J. M. Tranquada, V. Bisogni, and C. Mazzoli, [arXiv:2306.15086](https://doi.org/10.48550/arXiv.2306.15086) (2023), <https://doi.org/10.48550/arXiv.2306.15086>.
- [15] C. T. Parzyck, N. K. Gupta, Y. Wu, V. Anil, L. Bhatt, M. Bouliane, R. Gong, B. Z. Gregory, A. Luo, R. Sutarto, F. He, Y. D. Chuang, T. Zhou, G. Herranz, L. F. Kourkoutis, A. Singer, D. G. Schlom, D. G. Hawthorn, and K. M. Shen, *Nat. Mater.* (2024), <https://doi.org/10.1038/s41563-024-01797-0>.
- [16] X. Ren, R. Sutarto, Q. Gao, Q. Wang, J. Li, Y. Wang, T. Xiang, J. Hu, F. Zhang, J. Chang, R. Comin, X. J. Zhou, and Z. Z., [arXiv:2303.02865](https://doi.org/10.48550/arXiv.2303.02865) (2023), <https://doi.org/10.48550/arXiv.2303.02865>.
- [17] C. C. Tam, J. Choi, X. Ding, S. Agrestini, A. Nag, B. Huang, H. Luo, M. García-Fernández, L. Qiao, and K. J. Zhou, *Nat. Mater.* **21**, 1116 (2022).
- [18] F. Bernardini, L. Iglesias, M. Bibes, and A. Cano, *Front. Phys.* **10**, 828007 (2022).
- [19] D. Huang and J. E. Hoffman, *Annual Review of Condensed Matter Physics* **8**, 311 (2017), <https://doi.org/10.1146/annurev-conmatphys-031016-025242>.
- [20] Q. Y. Wang, L. Zhi, Z. Wen-Hao, Z. Zuo-Cheng, Z. Jin-Song, L. Wei, D. Hao, O. Yun-Bo, D. Peng, C. Kai, W. Jing, S. Can-Li, H. Ke, J. Jin-Feng, J. Shuai-Hua, W. Ya-Yu, W. Li-Li, C. Xi, M. Xu-Cun, and X. Qi-Kun, *Chinese Physics Letters* **29**, 037402 (2012).
- [21] D.-H. Lee, *Annual Review of Condensed Matter Physics* **9**, 261 (2018), <https://doi.org/10.1146/annurev-conmatphys-033117-053942>.
- [22] H. Y. Hwang, Y. Iwasa, M. Kawasaki, B. Keimer, N. Nagaosa, and Y. Tokura, *Nature Materials* **11**, 103 (2012).
- [23] A. Soumyanarayanan, N. Reyren, A. Fert, and C. Panagopoulos, *Nature* **539**, 509 (2016).
- [24] J. Pellicciari, S. Karakuzu, Q. Song, R. Arpaia, A. Nag, M. Rossi, J. Li, T. Yu, X. Chen, R. Peng, M. García-Fernández, A. C. Walters, Q. Wang, J. Zhao, G. Ghiringhelli, D. Feng, T. A. Maier, K.-J. Zhou, S. Johnston, and R. Comin, *Nature Communications* **12**, 3122 (2021), number: 1 Publisher: Nature Publishing Group.
- [25] J. Pellicciari, S. Lee, K. Gilmore, J. Li, Y. Gu, A. Barbour, I. Jarrige, C. H. Ahn, F. J. Walker, and V. Bisogni, *Nature Materials* **20**, 188 (2021), number: 2 Publisher: Nature Publishing Group.
- [26] S. Fan, H. Das, A. Rebola, K. A. Smith, A. Mundy, C. Brooks, M. E. Holtz, D. A. Muller, C. J. Fennie, R. Ramesh, D. G. Schlom, S. McGill, and J. L. Musfeldt, *Nat. Commun.* **11**, 5582 (2020).
- [27] G. Catalan, *Phase Transitions* **81**, 729 (2008).
- [28] J. A. Mundy, Y. Hikita, T. Hidaka, T. Yajima, T. Higuchi, H. Y. Hwang, D. A. Muller, and L. F. Kourkoutis, *Nat. Commun* **5**, 3464 (2014).
- [29] A. Ohtomo and H. Y. Hwang, *Nature* **427**, 423 (2004).
- [30] C. Yang, R. A. Ortiz, Y. Wang, W. Sigle, H. Wang, E. Benckiser, B. Keimer, and P. A. van Aken, *Nano. Lett.* **9**, 3291–3297 (2023).
- [31] B. H. Goodge, B. Geisler, K. Lee, M. Osada, B. Y. Wang, D. Li, H. Y. Hwang, R. Pentcheva, and L. F. Kourkoutis, *Nat. Mater.* **22**, 466 (2023).
- [32] A. Raji, G. Krieger, N. Viart, D. Preziosi, J. P. Rueff, and A. Gloter, *Small* **19**, 2304872 (2023).
- [33] B. Geisler and R. Pentcheva, *Phys. Rev. B.* **102**, 020502(R) (2020).
- [34] R. He, P. Jiang, Y. Lu, Y. Song, M. Chen, M. Jin, L. Shui, and Z. Zhong, *Phys. Rev. B.* **102**, 035118 (2020).
- [35] Y. Zhang, L. F. Lin, W. Hu, A. Moreo, S. Dong, and E. Dagotto, *Phys. Rev. B.* **102**, 195117 (2020).
- [36] F. Bernardini and A. Cano, *J. Phys. Mater* **3**, 03LT01 (2020).
- [37] M. Rossi, H. Lu, A. Nag, D. Li, M. Osada, K. Lee, B. Y. Wang, S. Agrestini, M. Garcia-Fernandez, Y. D. Chuang, Z. X. Shen, H. Y. Hwang, B. Moritz, K.-j. Zhou, T. P. Devereaux, and W. S. Lee, *Phys. Rev. B* **104**, L220505 (2021).
- [38] Y. Nomura and R. Arita, *Rep. Prog. Phys.* (2022), [10.1088/1361-6633/ac5a60](https://doi.org/10.1088/1361-6633/ac5a60).
- [39] S. W. Zeng, X. N. Yin, C. J. Li, C. L. E., C. S. Tang, K. Han, Z. Huang, Y. Cao, D. Y. Wan, Z. T. Zhang, Z. S. Lim, C. Z. Diao, P. Yang, A. T. S. Wee, S. J. Pennycook, and A. Ariando, *Nat. commun.* **13**, 743 (2022).
- [40] A. Botana, F. Bernardini, and A. Cano, *J. Exp. Theor. Phys.* **132**, 618–627 (2021).
- [41] Y. Ji, J. Liu, L. Li, and Z. Liao, *J. Appl. Phys.* **130**, 060901 (2021).
- [42] See Supplemental Information, which includes Refs 49–56, for additional information about the experimental methods, *dd* excitation assignments, fitting details, and details of the Density functional theory calculations.
- [43] S. Zeng, C. S. Tang, Z. Luo, L. E. Chow, Z. S. Lim, S. Prakash, P. Yang, C. Diao, X. Yu, Z. Xing, R. Ji, X. Yin, C. Li, X. R. Wang, Q. He, M. B. H. Breese, A. Ariando, and H. Liu, *Phys. Rev. Lett.* **133**, 066503 (2024).
- [44] B. H. Goodge, D. Li, K. Lee, M. Osada, B. Y. Wang, G. A. Sawatzky, H. Y. Hwang, and L. F. Kourkoutis, *Proceedings of the National Academy of Sciences* **118**, e2007683118 (2021), <https://www.pnas.org/content/118/2/e2007683118.full.pdf>.
- [45] M. Hepting, D. Li, C. J. Jia, H. Lu, E. Paris, Y. Tseng, X. Feng, M. Osada, E. Been, Y. Hikita, Y. D. Chuang, Z. Hussain, K. J. Zhou, A. Nag, M. Garcia-Fernandez, M. Rossi, H. Y. Huang, D. J. Huang, Z. X. Deann,

- T. Schmitt, H. Y. Hwang, B. Moritz, J. Zaanen, T. P. Devereaux, and W. S. Lee, *Nature Mater.* **19**, 381 (2020).
- [46] R. Coldea, S. M. Hayden, G. Aeppli, T. G. Perring, C. D. Frost, T. E. Mason, S. W. Cheong, and Z. Fisk, *Phys. Rev. Lett.* **86**, 5377 (2001).
- [47] M. Dantz, J. Pellicciari, D. Samal, V. Bisogni, Y. Huang, P. Olalde-Velasco, V. N. Strocov, G. Koster, and T. Schmitt, *Sci. Rep.* **6**, 32896 (2016).
- [48] K. Hu, Q. Li, D. Song, Y. Jia, Z. Liang, S. Wang, H. Du, H. Wen., and B. Ge., *Nat. Commun.* **15**, 5104 (2024).
- [49] Q. Gao, Y. Zhao, X. J. Zhou, and Z. Zhu, *Chin. Phys. Lett.* **38**, 077401 (2021).
- [50] Y. Li, W. Sun, J. Yang, X. Cai, W. Guo, Z. Gu, Y. Zhu, and Y. Nie, *Frontiers in Physics* **9**, 443 (2021).
- [51] R. Fumagalli, L. Braicovich, M. Minola, Y. Y. Peng, K. Kummer, D. Betto, M. Rossi, E. Lefrancois, C. Morawe, M. Salluzzo, H. Suzuki, F. Yakhou, M. Le Tacon, B. Keimer, N. B. Brookes, M. Moretti Sala, and G. Ghiringhelli, *Phys. Rev. B* **99**, 134517 (2019).
- [52] J. Q. Lin, H. Miao, D. G. Mazzone, G. D. Gu, A. Nag, A. C. Walters, M. García-Fernández, A. Barbour, J. Pellicciari, I. Jarrige, M. Oda, K. Kurosawa, N. Momono, K. J. Zhou, V. Bisogni, X. Liu, and M. P. M. Dean, *Phys. Rev. Lett.* **124**, 207005 (2020).
- [53] G. Kresse and J. Furthmüller, *Phys. Rev. B* **54**, 11169 (1996).
- [54] G. Kresse and J. Furthmüller, *Computational Materials Science* **6**, 15 (1996).
- [55] P. Blaha, K. Schwarz, F. Tran, R. Laskowski, G. K. H. Madsen, and L. D. Marks, *The Journal of Chemical Physics* **152** (2020), 10.1063/1.5143061, 074101, https://pubs.aip.org/aip/jcp/article-pdf/doi/10.1063/1.5143061/16727313/074101_1.online.pdf.
- [56] J. P. Perdew, K. Burke, and M. Ernzerhof, *Phys. Rev. Lett.* **77**, 3865 (1996).